4. ANALYSIS OF THE INVENTORIES

Super competence
is worst than incompetence.

The cost of an expertise is proportional
to the number of words you understand.

The information shown on landslide inventories can be used for a variety of analyses, including: (i) investigating landslide spatial abundance, through the production of landslide density maps; (ii) comparing inventory maps obtained from different sources (e.g., archive and geomorphological) for the same area; (iii) evaluating the completeness of the inventories; (iv) ascertaining landslide geographical persistence, by comparing event and geomorphological inventories; (v) estimating the frequency of slope failure occurrence, by analysing historical catalogues of landslide events or multi-temporal inventory maps; (vi) obtaining the statistics of landslide size; (vii) ascertaining landslide susceptibility and hazards, including the validation of the obtained susceptibility and hazard forecasts; (viii) determining the possible impact of landslides on built-up areas or the infrastructure; and (ix) contributing to establish levels of landslide risk. The quality and reliability of the different analyses obtained from a landslide inventory depend largely (often entirely) on the quality and completeness of the original landslide map. For this reason, one should always: (i) aim at compiling accurate and precise inventories, (ii) document the sources of information used to obtain the inventories, (iii) accurately describe the techniques, methods and tools used to prepare or compile the inventories, and (iv) try to assess the completeness of the obtained inventories. Limitations of landslide inventories should always be known (i.e., explicit and clear) to the users of the maps or the archives.

In this chapter, I discuss some of the possible applications of landslide inventories. I first demonstrate the construction and use of landslide density maps. I then show methods to compare geomorphological and historical inventories. I discuss an index to quantify the degree of matching between inventories, and I show an application for the comparison of the three landslide maps available for the Collazzone study area. I further discuss the issue of the completeness of the landslide inventories, and I use two event inventories available for Umbria to investigate geographical landslide persistence. Finally, I show how to ascertain the temporal frequency of slope failures from archive inventories.

4.1. Landslide abundance

To quantify the geographical (spatial) abundance of landslides, landslide density maps can be prepared. Landslide density (or frequency) maps measure the spatial distribution of slope

failures (Campbell, 1973; Wright *et al*., 1974; DeGraff, 1985; DeGraff and Canuti, 1988). Landslide density is the proportion (i.e., frequency, percentage) of landslide area, and is commonly computed as:

$$D_L = \frac{A_L}{A_M},\ 0 \le D_L \le 1 \tag{4.1}$$

where, A_M is the area of the mapping unit used to compute the density (e.g., grid cell, slope unit, unique condition unit, etc., see § 6.2.2), and A_L is the total landslide area in the mapping unit. In each mapping unit landslide density varies from 0, for landslide free units, to 1, where the entire unit is occupied by landslides.

Density maps have different applications. They have been used to: (i) show a synoptic view of landslide distribution for large regions or entire nations (Radbruch-Hall *et al.,* 1982; Reichenbach *et al.,* 1998a; Guzzetti *et al*., 2003), (ii) portray a first-order overview of landslide abundance (Campbell, 1973; Wright *et al.,* 1974; Wright and Nilsen, 1974; Pomeroy, 1978; Moreiras, 2004), (iii) show the magnitude of slope failures triggered by severe storms (Campbell, 1975; Ellen and Wieczorek, 1988), (iv) evaluate landslide abundance or landslide activity in relation to forest management, agricultural practise, and land use changes (DeGraff, 1985; DeGraff and Canuti, 1988), (v) show the spatial distribution of the historical frequency of rock fall events (Chau *et al*., 2003), and (vi) as a week proxy of landslide susceptibility (Bulut *et al*., 2000; Guzzetti *et al*., 2005d).

Landslide density maps are filler of space. This is different from inventory maps, which provide information only where landslides were recognized and mapped (§ 9.1). Density maps provide insight on the expected (or inferred) occurrence of landslides in any part of the investigated area without leaving unclassified areas. A density map does not show were landslides are located, but this loss in resolution is compensated for by improved map readability and reduced cartographic errors (Carrara *et al.,* 1992; Ardizzone *et al.,* 2002). Additionally, landslide density is independent of the extent of the study area, which makes comparison between different regions straightforward. Such characteristics make density maps appealing to decision-makers and land developers (§ 9.2).

Depending on the type of mapping unit used to compute and portray the density, landslide density maps can be based on statistical or geomorphological criteria (Guzzetti *et al.*, 2000).

4.1.1. Statistical landslide density maps

In statistically-based density maps, the mapping unit is usually an ensemble of grid cells (i.e., pixels), square or nearly circular in shape, with a size generally 10 to 100 times larger than the size of the individual grid cell (Guzzetti *et al.*, 2000). Density is determined by counting the percentage of landslide area within the mapping unit (in this case an artificial "kernel"), which is moved systematically across the territory. This is equivalent to a moving average filtering technique. Additional filtering or weighting techniques can be applied to improve map consistency and readability. By interpolating equal quantity (isopleth) lines, a statistically-based density map can be portrayed as a contour map (Wright *et al.,* 1974). The latter was the favoured method for showing landslide density (Campbell, 1973, 1975; Wright and Nielsen, 1974; DeGraff, 1985) before GIS technology and raster colour display were largely available.

Statistically-based landslide density maps rely on the assumption that landslide occurrence is a continuous variable that can be spatially interpolated (Schmid and MacCanell, 1955; Wright *et*

al., 1974; Guzzetti *et al.,* 1999a). Hence, they perform best in homogeneous terrain – where lithology and morphology do not change abruptly. This assumption is strong (geomorphologically) and holds true only as a general approximation – at small scale – and in homogeneous physiographic environments (Guzzetti *et al.*, 2000). At larger scales, the assumption of spatial continuity does not take into account the existing relations between slope failures and the local morphological, geological or land use settings. As an example, where layered rocks crop out, slope forms and processes are influenced by the attitude of bedding planes. In susceptible geologic environments, landslides are often larger and more abundant where bedding dips toward the slope free face. Conversely, where bedding dips into the slope (reverse slope) terrain is steep and landslides are less abundant (e.g., Guzzetti *et al.,* 1996b). In such conditions, an isopleth map prepared without considering the presence of streams or divides will be misleading, particularly on reverse slopes. This limitation is partly overcome by selecting a mapping unit that bears a physical relation to the geomorphology of landsliding (Carrara *et al.,* 1995; Guzzetti *et al.,* 1999a).

4.1.2. Geomorphological landslide density maps

For geomorphological density maps, slope units (as defined in Carrara *et al.,* 1991, see § 6.2.2) appear to be particularly suited to the determination of landslide spatial frequency. This subdivision of the terrain partitions the territory into domains bounded by drainage divides and stream lines. To delineate the divide and stream networks, manual techniques or automatic selection criteria can be adopted. The latter is based on the analysis of a digital terrain matrix (DTM) that acts as a computerised representation of topography (Carrara, 1988; Carrara *et al.,* 1991). Slope units, therefore, correspond to the actual slopes on which landslides take place. The percentage of landslide area within each slope unit, as counted, is equivalent to the percentage of failed area on each slope (see equation 4.1 and Figure 4.1). The landslide density in this case, is the proportion or percentage of the slope unit that is occupied by the landslides.

As they are delimited by morphological boundaries, slope units avoid the pitfall of forecasting high landslide densities in areas that are mapped as essentially landslide free but are close to known failures (for example, across the divide of an asymmetric ridge which is controlled by the attitude of bedding planes). In addition, slope units mitigate the effects of possible identification and mapping errors. As landslide density is computed for the entire mapped area, possible mapping or drafting errors made within each slope unit are averaged.

The advantage of morphologically soundness and the limitation of mapping errors are counterbalanced by the loss of resolution (Figure 4.1). The resolution of slope-unit based density maps is lower than that of grid based or contour based maps, unless the grid or contour spacing is particularly large for the amplitude of the terrain under study. As a result of interpolation procedures, landslide density is a derivative of the spatial distribution of landslides (i.e., the inventory). Interpolation inevitably causes information to be lost. Indeed, even if landslides were mapped in great detail, nothing could be said about the exact location of any single landslide within a slope unit. However, if the size of slope units is chosen in relation to the size of landslides to be studied, the loss of resolution is only apparent and does not correspond to a loss in the applicability and utility of the map (Carrara *et al.*, 1992, 1995, 1999; Guzzetti *et al.,* 1999a, 2000).

Errors and inconsistencies associated with the definition of slope units from DTMs, to the geometrical consistency between slope units and landslide boundaries, to the size of slope

units compared to the extent of landslide deposits, and to the correspondence between slope units and the actual geometry of the slopes, may limit the use of such mapping unit to properly count and display landslide density.

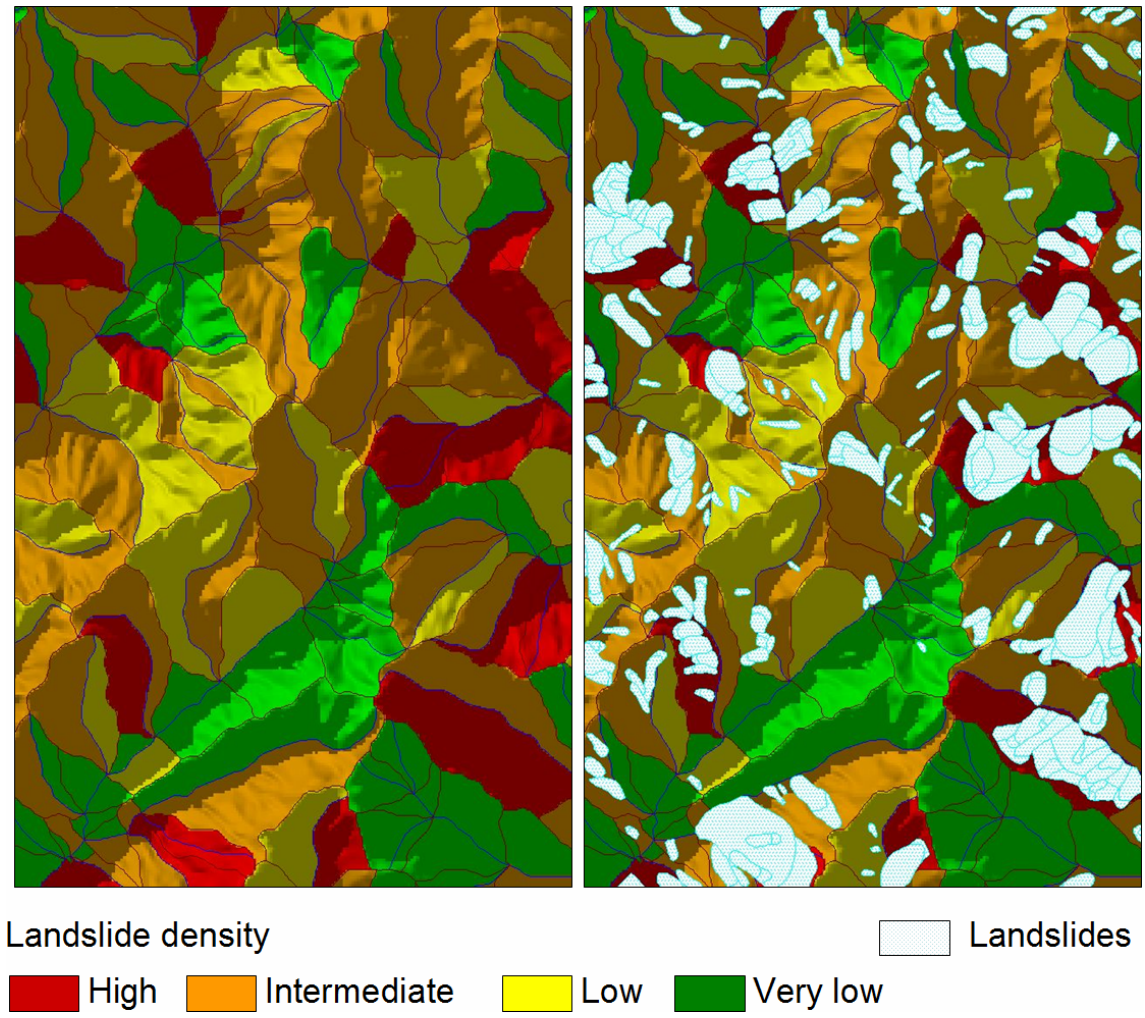

Figure 4.1 – Portion of a slope unit based geomorphological landslide density map for the Upper Tiber River basin, central Italy (Guzzetti *et al.*, 2000) (§ 2.3). Left map shows landslide density, in 4 classes, obtained by counting the percentage of landslide area within each slope unit. Right map was obtained by superimposing the landslide inventory and the density map. Agreement between the density and the inventory maps is apparent.

Other geomorphological mapping units (§ 6.2.2) can be used to compute and display landslide density. In general, the result is similar to that obtained using the slope units. Advantages and limitations of the different terrain partitioning methods depend largely on the aptitude of the selected type of unit to capture the complexity of the terrain, the available thematic information, and the pattern, distribution and abundance of landslides.

4.2. Comparison of landslide inventories

Two or more landslide inventories may be available for the same area. In this fortunate case, qualitative (heuristic) and quantitative (measurable) comparisons between the inventories are

possible. As an example of a qualitative approach, I compare two landslide inventories available for Umbria, namely the detailed geomorphological landslide inventory (Figure 3.10), and the historical archive inventory (Figure 3.4). Next, I discuss a method – originally proposed by Carrara *et al.* (1992) – for the quantitative comparison of two landslide maps, and I apply the method to the comparison of the three landslide inventories available for the Collazzone area (Figure 3.14).

4.2.1. Comparison of archive and geomorphological inventory maps

In Umbria, the historical archive inventory (§ 3.3.1.1) and the detailed geomorphological landslide inventory (§ 3.3.2.2) provide different and complementary pictures of the distribution, pattern and density of landslide phenomena. The detailed geomorphological inventory shows the sum of many landslide events that occurred in Umbria over a period of hundreds or thousands of years (Guzzetti *et al.*, 2003). Analysis of the geomorphological mapping indicates that total landslide area in the region is 712.64 km^2 (8.4%), of which 519.12 km^2 is in the Perugia province (8.2%) and 192.52 km^2 in the Terni province (9.1%). This is a minimum estimate because an unknown number of landslides were removed by erosion, human activities and growth of vegetation, and small landslides may have not been recognized in the aerial photographs or in the field. Figure 4.2.A shows the percentage of landslide area in the 92 Municipalities of the region. The percentage of landslide area varies from 0% (Bastia, in green) to more than 30% (Allerona, 33.9%, Penna in Teverina, 35.4%, in light blue).

For the Umbria region, the national archive of historical landslide events (§ 3.3.1.1) covers the period from 1917 to 2001 and reports information on 1292 landslide sites, affected by a total of 1488 landslide events (Figure 3.4). This is equivalent to 1.5 landslide sites per 10 square kilometres in 85 years. Landslide events were reported in 90 of the 92 Municipalities in the region (97.8%). Figure 4.2.B shows the number of sites affected by historical landslides in each Municipality. The number of landslide sites ranges from 0, where no historical information was reported, to 116, for the Perugia Municipality. The latter is equivalent to an average of 1.4 damaging landslide events per year.

Comparison of the two inventories is not straightforward. Of the eight Municipalities with less than 2% of landslide area (green in Figure 4.2.A), six (75%) experienced only a few (≤ 5, green in Figure 4.2.B) historical landslide events in the 85-year period between 1917 and 2001. In these Municipalities the two inventories provide consistent information. However, of the 13 Municipalities exhibiting 15% or more landslide area (light blue in Figure 4.2.A), according to the historical catalogue only one (Pietralunga) has experienced a very large number of landslide events (>25, red in Figure 4.2.B). This is less consistent, and shows that the technique used to compile an inventory affects the obtained analysis of the distribution and density of the landslides.

The observed differences are justified by the different type of information shown by the two inventories. Lack or abundance of landslides in the geomorphological inventory map depends largely on the local lithological and morphological setting. Abundance of historical information on landslide events depends on many factors, including the availability of historical sources, the density and distribution of the population, the built-up areas, the infrastructure, and other vulnerable elements. Due to the technique used to collect the information, the historical archive is certainly incomplete. Landslide events listed in the historical catalogue tend to concentrate in the towns and villages and along the roads (Guzzetti *et al.*, 1994; Guzzetti and Tonelli, 2004). It is therefore possible that landslides occurred in

places and were not reported. Slope failures occurred in remote or distant areas may have not been noticed by the population. Alternatively, they may have been observed but quickly removed, or they may have not been reported because they did not cause significant damage.

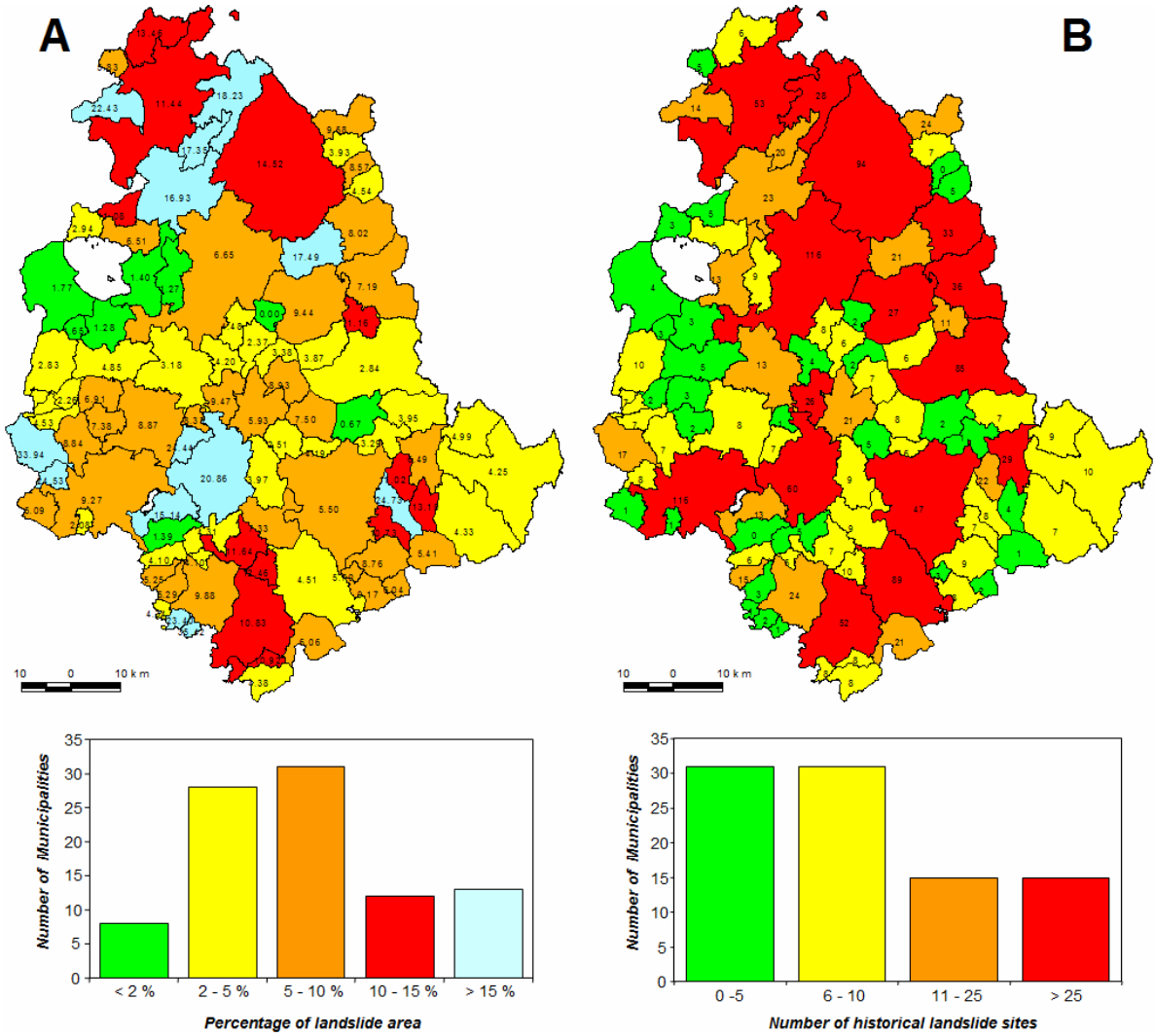

Figure 4.2 – Umbria Region. Comparison of geomorphological and historical inventory maps. (A) Percentage of landslide areas in the 92 Municipality obtained from the detailed geomorphological landslide inventory (see § 3.3.2.2). Histogram shows number of Municipalities in five classes of the percentage of landslide area. (B) Number of historical landslide sites in each Municipality obtained from the archive inventory (see § 3.3.1.1). Histogram shows abundance of Municipalities in four classes of number of historical landslide sites.

4.2.2. Comparison of two geomorphological landslide inventory maps

Only a few authors have attempted to quantitatively compare geomorphological landslide inventory maps (Roth, 1983; Carrara *et al.*, 1992; Ardizone *et al.*, 2000; Galli *et al.*, 2005). Carrara *et al.* (1992) proposed a quantitative and reproducible method for comparing two landslide inventory maps. For the purpose, these authors introduced an index to measure the degree of mismatch between two inventory maps. The mismatch (or error) index, *E*, is given by:

$$E = \frac{(A'_{LT} \cup A''_{LT}) - (A'_{LT} \cap A''_{LT})}{(A'_{LT} \cup A''_{LT})},\ 0 \le E \le 1 \tag{4.2}$$

Where, A'_{LT} and A''_{LT} are the total landslide area in the first and in the second inventory, respectively, and $\cup$ and $\cap$ are the geographical union and intersection of the two inventories, easily obtained in a GIS.

From equation 4.2, the degree of matching, *M*, between two inventory maps can be obtained as:

$$M = 1 - E,\ 0 \le M \le 1 \tag{4.3}$$

If two landslide inventory maps portray exactly the same landslides (a rather improbable situation), $E = 0$ and $M = 1$, i.e., matching is perfect and mismatch is nil. If the two inventory maps disagree completely, $E = 1$ and $M = 0$, i.e., cartographic matching is nil and mismatch is maximum.

Figure 4.3 shows a comparison of two geomorphological inventory maps prepared for the La Honda area, in the San Francisco Bay region, used by Carrara *et al.* (1992) to investigate uncertainties associated with landslide inventory making. In this experiment, GIS technology was used to determine and quantitatively compare the effect of mapping errors produced by different causes in the compilation of inventory maps from the interpretation of aerial photographs.

Three tests were performed. The first test consisted in comparing two geomorphological landslide inventory maps produced independently by two equally experienced interpreters, which mapped landslides in the La Honda area using black-and-white, 1:18,000 scale aerial photographs and 1:24,000 scale base maps (Figure 4.3, left map). Before starting the operation, one of the two investigators had the opportunity to visit the area. Visual inspection of the maps produced by the two separate investigators indicates that the overall spatial distribution of landslides in the two maps is fairly similar. The percentages of landslide area were 13.5% and 16.8%, for the first and the second investigator, respectively. GIS analysis revealed that 9.9% of the total landslide area was common to both maps (geometrical intersection), and that 20.3% of the area was classified as bearing landslides by either the first or the second interpreter (geometrical union). The mismatch error computed with equation 4.2 was 51.5%, corresponding to a cartographic matching (eq. 4.3) of (only) 48.5%.

An attempt was made to separate the errors caused by differences in investigators' interpretation and judgement from other sources of errors, including inaccuracies in topographic data location, and data restitution, drafting, digitization and construction of the GIS database. For the purpose, a buffer was traced around each mapped landslide in both inventories. The operation was repeated four times, using buffers of 25, 50, 100 and 200 m width. Results (Figure 4.3, right graph) indicated that first the error decreased at a slow rate, and then it declined more rapidly, and (almost) linearly. Because of the scale of the base maps (1:24,000) and of the aerial photographs (1:18,000) used for the investigation, and the standard inaccuracy in data digitizing and storing landslide information in the GIS database, the total error associated with such operations was accounted by a buffer of approximately 50 m in width. This leaded to an error of approximately 5% (Figure 4.3, right graph). The remaining error (approximately 46%) represented the actual mismatch due to the different geomorphological interpretations performed by the two investigators.

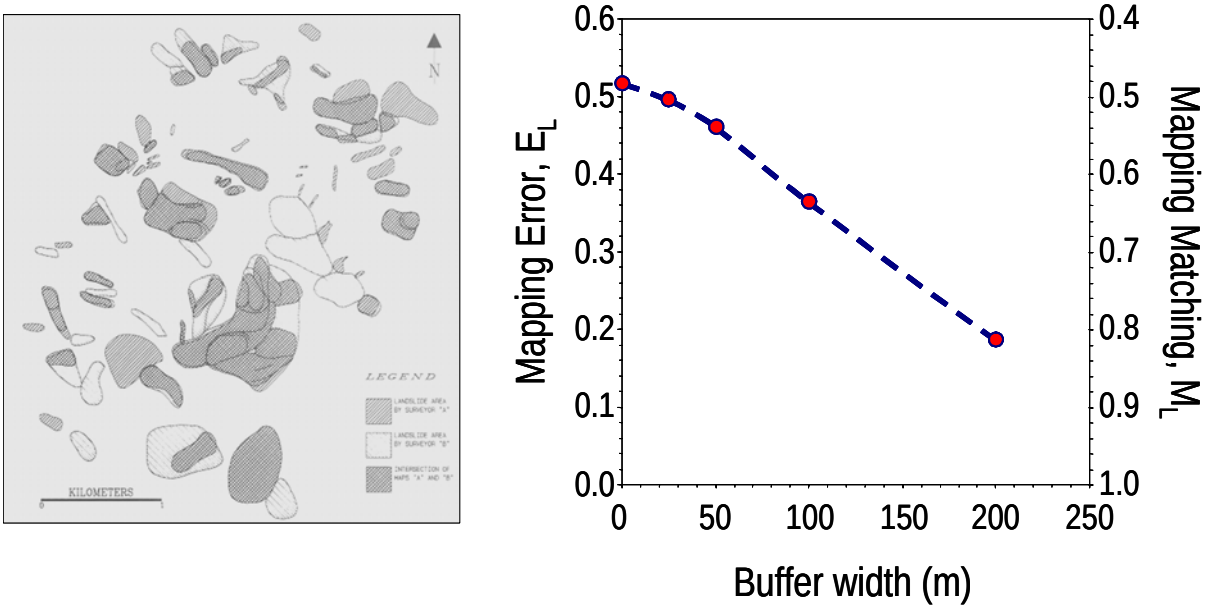

Figure 4.3 – La Honda study area, California. Left map, geographical comparison of two geomorphological landslide inventory maps. Right graph, estimated mapping and mismatch indexes obtained by adding uncertainty buffers of different width, from 0 to 200 m. Modified after Carrara *et al*. (1992).

The second test was aimed at comparing two geomorphological landslide inventory maps produced by the same team of two geomorphologists – of whom one was I – for the same area, using two different sets of aerial photographs and the same stereoscopes. The test was conducted in the Tescio River basin, which extends for about 60 km^2 in central Umbria. The first inventory was the reconnaissance regional mapping of Umbria (§ 3.3.2.1, Figure 3.9). The second inventory was a detailed geomorphological mapping prepared at 1:10,000 scale through the interpretation of 1:13,000 scale colour aerial photographs flown in 1977, supplemented by extensive geological and geomorphological field mapping (Carrara *et al.*, 1991). The new geomorphological inventory was prepared after the reconnaissance map was completed, and benefited from the re-interpretation of the 1:33,000 scale aerial photographs.

The reconnaissance mapping identified 15.4% of the Tescio basin as having a landslide. The following detailed geomorphological maps identified 12.8% of the basin as being affected by slope failures. The reduced percentage of landslide terrain in the second inventory is justified by a more accurate mapping, particularly of the largest landslides. GIS analysis revealed that 7.8% of the total landslide area was common to both maps (geometrical intersection), and 20.4% of the area was classified as having landslides in both inventories (geometrical union). Hence, the computed mapping error was 61.8%, and the cartographic matching was 38.2%.

The third test compared landslide maps produced independently by two different teams, using different resources (i.e., aerial photographs, stereoscopes, base maps, time, etc.) and for different scopes. For the test, a portion of the Marecchia River basin, in the northern Apennines, was selected. The area, which extends for 46 km^2, consists of clayey terrains very prone to landslides. Most of the slope failures are old, dormant-to-active flows or slide-flows (Guzzetti *et al.*, 1996). For this area, the first inventory was produced by the Emilia-Romagna Region Geological Survey as part of a regional reconnaissance mapping project carried out in

the late 1970s. Landslides were mapped using aerial photographs (of unknown scale), base maps at 1:25,000 scale, and field investigations. No information was available about the experience of the team that prepared the first inventory. The same area was remapped by the team of geomorphologists who prepared the maps used in the second test. These investigators used 1:33,000 scale aerial photographs flown in the period from 1954 to 1955, 1:25,000 scale base maps, and some field checks. The first mapping identified 8.1% of the study area as having a landslide. The second inventory identified 10.3% of the study area as having a landslide. GIS analysis revealed that only 3.3% of the total landslide area was common to both maps (geometrical intersection), and that 15.1% of the study area was classified as having a landslide in both inventories (geometrical union). The resulting cartographic error was particularly large, 77.9%, and the cartographic matching was correspondingly reduced to 22.1%.

The described method to quantitatively compare two landslide inventory maps is particularly severe. Even a (apparently) minor discrepancy in the mapping results in a considerable mapping error. The test is also somewhat imprecise. The test considers the total landslide area, and mapping errors made in different parts of the two maps may compensate. Also, differences in the classification of landslide types are not considered. The test can only be applied to compare two inventories ("pair-wise" comparison), and extension to three or more inventory maps is impractical, albeit it has been attempted (Galli *et al*., 2005).

Further, Figure 4.4 shows that the test is not capable of distinguishing where the same landslide is mapped in two completely different (disjoint) areas (A), from where one of the two maps portrays a landslide and the other map does not show it (B). The two cases have a different connotation in terms of the correctness of the mapping. Finally, the test does not provide direct insight on the quality of the mapping. Referring to Figure 4.3, the test indicates the degree of matching (or mismatching) between the two maps, but does not provide any insight on the veracity of the mapping, i.e., which of the two maps is correct in identifying landslides, and where. This can only be decided using external information.

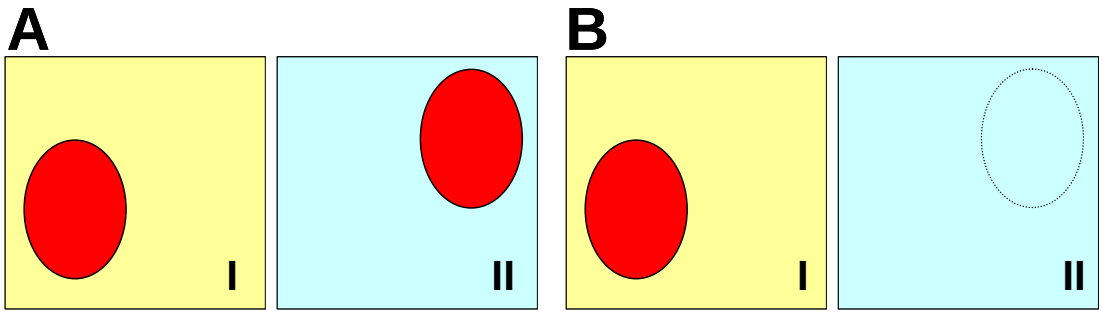

Figure 4.4 – Problems with index that measures the degree of mismatch between two inventory maps. (A) Landslide mapped in two different positions by two interpreters; $E = 1$ and $M = 0$. (B) One map shows the landslide and the other map does not. Similarly to the previous case, $E = 1$ and $M = 0$. The two types of mapping errors are different, but the index provides the same result.

Despite the clear limitations, the discussed method – and the associated indexes – remains a useful, simple and practical way of comparing two landslide inventory maps. Applying remote sensing classification techniques (e.g., Cohen, 1960; Hoehler, 2000; Pontius, 2000; Pontius, personal communication, 2001), or standard forecast verification methods (e.g., Jollifee and Stephenson, 2003), improvements to the proposed method are certainly possible.

4.2.2.1. Further comparison of the landslide maps in the Collazzone area

In this section, I continue the analysis of the three inventory maps available for the Collazzone area (Figure 3.14). More precisely, adopting the previously describe method I attempt to determine the degree of cartographic matching (and mismatching) among the three landslide maps. For the purpose, in a GIS I performed pair-wise geometrical intersection ($\cap$) and union ($\cup$) of the three landslide maps. Then, I use the obtained figures to compute the error (E) and matching (M) indexes. Results of this analysis are summarized in Table 4.1.

Table 4.1 – Comparison of landslide inventory maps in the Collazzone area. Mapping error, E, and mapping mismatch, M, computed using equations (4.2) and (4.3), respectively. Map A, reconnaissance landslide inventory (§ 3.3.2.1). Map B, detailed geomorphological inventory (§ 3.3.2.2). Map C, multi-temporal inventory (§ 3.3.4.1).

Landslide area in Map A (reconnaissance geomorphological inventory)	%	9.73
Landslide area in Map B (detailed geomorphological inventory)	%	10.05
Map A $\cup$ Map B	%	16.75
Map A $\cap$ Map B	%	3.18
Mapping error, E	-	0.81
Mapping match, M	-	0.19
Landslide area in Map A (reconnaissance geomorphological inventory)	%	9.73
Landslide area in Map C (multi-temporal inventory)	%	20,69
Map A $\cup$ Map C	%	24.86
Map A $\cap$ Map C	%	5.71
Mapping error, E	-	0.77
Mapping match, M	-	0.23
Landslide area in Map B (detailed geomorphological inventory)	%	10.05
Landslide area in Map C (multi-temporal inventory)	%	20.69
Map B $\cup$ Map C	%	22.93
Map B $\cap$ Map C	%	7.81
Mapping error, E	-	0.66
Mapping match, M	-	0.34

Inspection of Table 4.1 indicates that overall mapping error (E) ranges from 0.66 to 0.81, which corresponds to a degree of map matching (M) in the range between 0.34 and 0.19, respectively. As expected, overall mapping error is smallest (0.66) when the most accurate (i.e., the multi-temporal inventory, "Map C") and the second most accurate (i.e., the detailed geomorphological inventory, "Map B") inventories are compared.

As I have shown previously, an attempt can be made to separate the drafting and digitization errors from the mismatch due to different geomorphological interpretations of the actual ("real") landslide distribution. To accomplish this, in the GIS I draw buffers of 1 m, 3 m, 5 m, 10 m, 20 m and 100 m around the landslides shown in the detailed inventory maps (i.e. the detailed regional inventory, § 3.3.2.2, and the multi-temporal inventory, § 3.3.4.1), which were both originally obtained at 1:10,000 scale, and buffers of 2.5 m, 7.5 m, 12.5 m, 25 m, 50 m and 250 m around the landslides shown in the reconnaissance inventory map (§ 3.3.2.1),

which was originally prepared at 1:25,000 scale. The selected buffers correspond to 0.1 mm, 0.3 mm, 0.5 mm, 1.0 mm, 2.0 mm and 10 mm, respectively, on the base maps used to show the landslide information. Results of the GIS analysis are shown in Figure 4.5. With increasing buffer size, mapping error (*E*) first decreases at a slow rate and then, for large buffers, it decreases rapidly (Figure 4.5.A). Conversely, map matching (*M*) first increases slowly and then rapidly (Figure 4.5.B).

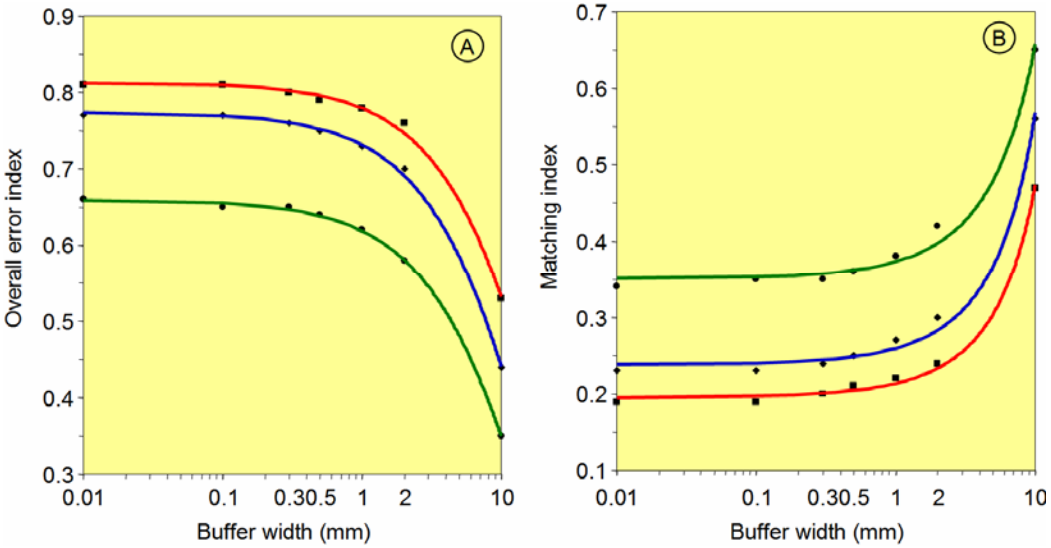

Figure 4.5 – Collazzone area. Estimate of overall mapping errors (A) and map matching indexes (B) for three pair wise combinations of landslide inventory maps. Squares, Map A and Map B in Table 4.1; diamonds, Map A and Map C in Table 4.1; dots, Map B and Map C in Table 4.1. Lines show exponential fits to the data (least square method).

The geometric error resulting from inaccuracies in transferring the landslide information from the aerial photographs to the base maps and the digitization errors can be accounted for by a buffer of about 10 m for the more detailed inventories (§ 3.3.2.2, § 3.3.4.1), and by a buffer of about 50 m for the reconnaissance inventory map (§ 3.3.2.1). These figures correspond to a cartographic error of approximately 2.5 - 5.0%. The remaining mismatch (~ 62% - 75%) can be attributed to different (i.e., relevant, significant) geomorphological interpretations of the landslides. This is relevant information for the assessment of landslide hazard.

To further investigate the differences between the three landslide maps, I examined the differences in the abundance of slope failures shown by the three maps. To obtain this, I first partitioned the study area into slope units, i.e., portions of the terrain delimited by drainage and divide lines (see § 6.2.5). For each slope unit, I computed in the GIS the percentage of landslide area (i.e., the density) shown in the three landslide inventories. Results are shown in Figure 4.6. Inspection of this Figure indicates that the geographical distribution of landslide density (abundance) varies considerably for the three inventory maps. This is not surprising given the original distribution of the slope failures in the three landslide maps (Figure 3.14).

Visual comparison of the inventory (Figure 3.14) and the density (Figure 4.6) maps suggests that slope units having a proportion of landslide area of less than about 3% can be considered free of landslides (i.e., stable). I select this – empirical – cut-off value to account for all the drafting and cartographic errors. Inspection of the original landslide maps in the GIS reveals that, typically, such errors are represented by a small portion of a landslide deposit crossing a stream line or a divide.

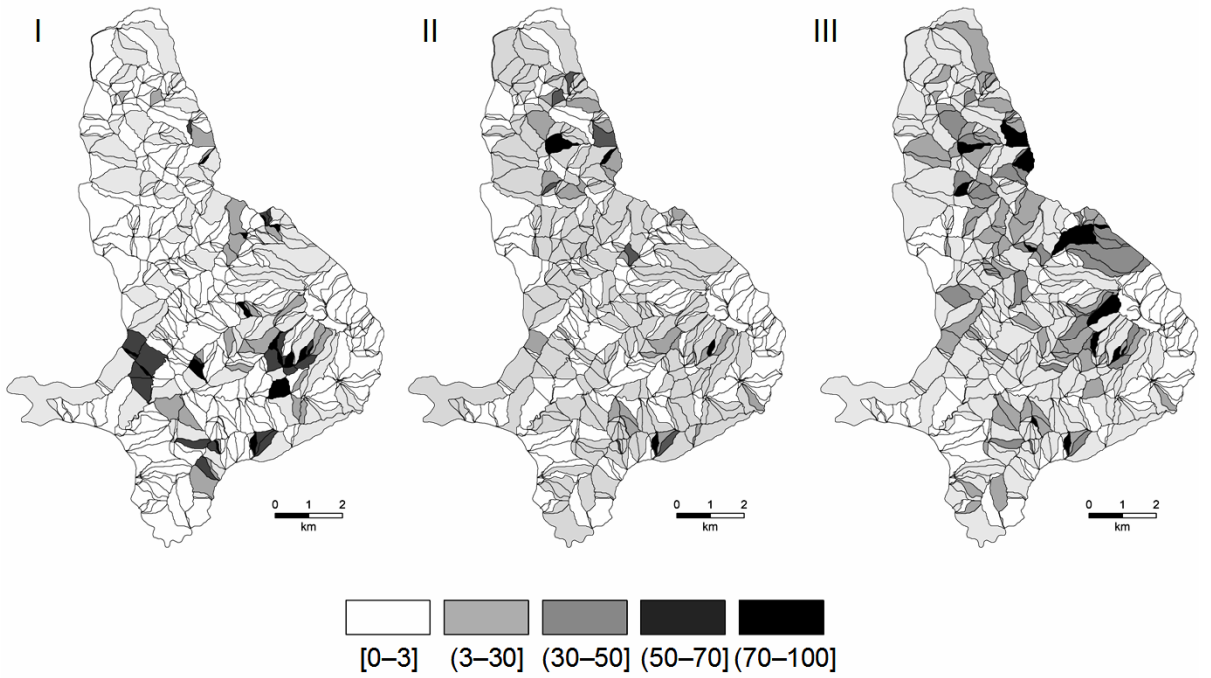

Figure 4.6 – Landslide density maps for the Collazzone area. (I) reconnaissance geomorphological inventory (§ 3.3.2.1), (II) detailed geomorphologic inventory (§ 3.3.2.2), (III) multi-temporal inventory (§ 3.3.4.1). See Figure 3.14 for comparison. Landslide density computed within slope units. Slope units with a percentage of landslide area of less than 3% are considered stable and shown in white. Shades of grey indicate different landslide density. In the legend, square bracket indicates class limit is included, and round bracket indicates class limit is not included.

In Figure 4.6, there are 358 stable terrain units (in white) in the density map obtained from the reconnaissance geomorphological inventory (Map I), 255 stable units in the density map obtained from the detailed geomorphological inventory (Map II), and only 153 stable units in the density map obtained from the multi-temporal inventory (Map III). Reduction in the number of stable terrain units is due to a better accuracy of the landslide mapping, which resulted in the identification of a larger number of mass movements.

To better analyse the degree of matching (or mismatching) between the three density maps shown in Figure 4.6, I performed pair-wise comparisons of the maps in the GIS and I constructed specific contingency tables (Table 4.2). The least disagreement (33.3%) is observed when comparing the densities obtained from the "best" (Map C) and the second "best" (Map B) landslide maps, respectively. The comparison outlines a similarity between these two density maps (e.g., Map III and Map II). Mismatch between Map I and Map II, and between Map I and Map III in Figure 4.6 is very similar (~ 62%), confirming that the density map obtained from the reconnaissance inventory (Map A) is substantially different from the other two density maps.

Figure 4.7 summarizes the results of the performed pair-wise comparisons. There are 242 terrain units (47.1%) classified as stable (130 slope units, 25.3%) or unstable (112 slope units, 21.8%) by all three density maps. These terrain units represent perfect agreement between the three density assessments. There are 429 slope units (83.5%) for which the density obtained from Map A or Map B is in agreement with the density obtained from Map C, considered the "best" available landslide map.

Table 4.2 – Collazzone area. Comparison of stable and unstable slope units based on landslide density computed for the three landslide inventory maps. Stable slope units have a percentage of landslide area of less than 3 percent. Figures in the tables indicate number of terrain units. Map I, density map shown in Figure 4.6.I and obtained from the reconnaissance inventory (§ 3.3.2.1, Figure 3.14.A). Map II, density map shown in Figure 4.6.II and obtained from the detailed geomorphological inventory (§ 3.3.2.2, Figure 3.14.B). Map III, density map shown in Figure 4.6.III and obtained from the multi-temporal inventory (§ 3.3.4.1, Figure 4.6.III).

		Map I	
		Stable (358)	Unstable (156)
Map II	Stable (255)	213	42
	Unstable (259)	145	114

Disagreement between the density maps I and II = 62.12 %

		Map I	
		Stable (358)	Unstable (156)
Map III	Stable (153)	139	14
	Unstable (361)	219	142

Disagreement between the density maps I and III = 62.13 %

		Map II	
		Stable (255)	Unstable (259)
Map III	Stable (153)	142	11
	Unstable (361)	113	248

Disagreement between the density maps II and III = 33.33 %

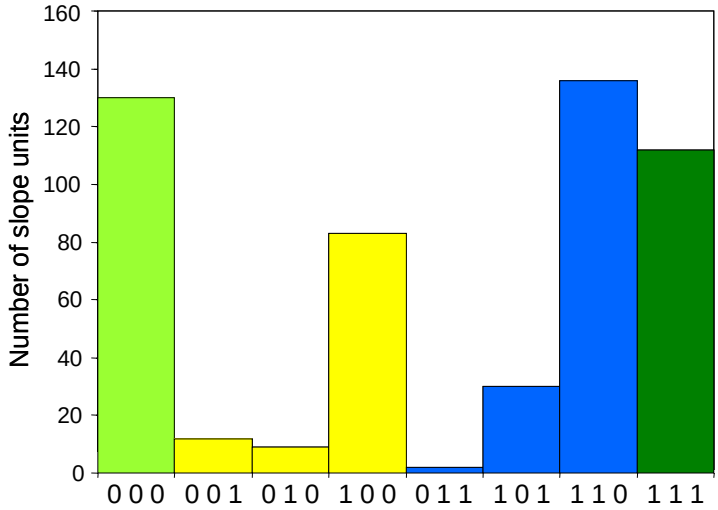

Figure 4.7 – Comparison of stable (0) and unstable (1) slope units based on landslide density in the Collazzone area. Stable slope units have a percentage of landslide area < 3%. Legend of the vertical bars (x-axis): left digit is the multi-temporal inventory (Map C), central digit is the detailed geomorphological inventory (Map B), and right digit is the reconnaissance inventory (Map A).

Lastly, I compared the percentage of landslide area attributed to each slope unit by the single density maps (Figure 4.8). Comparison of the density obtained from the "best" (Map C) and the "poorest" (Map A) landslide maps resulted in the largest scatter (central graph in Figure 4.8). A considerable number of slope units exhibiting a small density of landslides in Map I show a large proportion of landslides in Map III, and vice versa. This is an indication that the geographical distribution of the landslides shown in the two inventories is significantly different. Comparison of the density Map II (obtained form the geomorphological inventory) with the density Map III (obtained form the multi-temporal inventory) indicates that the differences are largely due to the absence in the geomorphological inventory of several large and very large landslides (Figure 3.14).

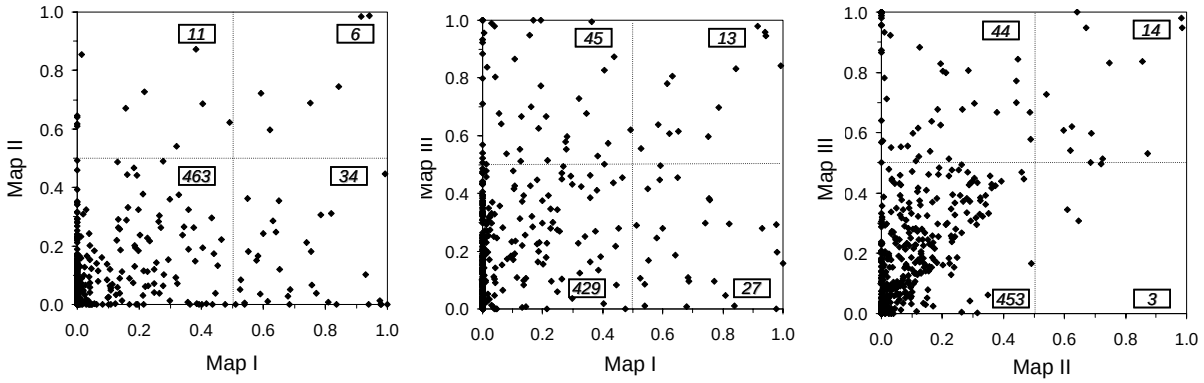

Figure 4.8 – Comparison of landslide density in the slope units in the Collazzone area. Left graph shows comparison of Map I and Map II in Figure 4.6. Central graph shows comparison of map I and map III. Right graph shows comparison of Map II and Map III.

In conclusion, the density maps obtained from the three landslide inventories available for the Collazzone area (Figure 3.14) provide different descriptions of the propensity of the area to experience new or reactivated landslides. Base on these findings, I conclude that the landslide density obtained from the multi-temporal map (Map III in Figure 4.6) is a reliable description of the abundance of slope failures in the Collazzone area. I also conclude that, in the Collazzone area, the detailed geomorphological inventory provides a better description of landslide abundance than the reconnaissance landslide mapping. These finding are relevant to the assessment of landslide susceptibility and hazards at the regional scale in Umbria.

This does not conclude the comparative analysis of the quality of the landslides maps available for the Collazzone area. In § 5.3.1 I will compare the frequency-area statistics obtained for the three inventories, and I will use the obtained finding to infer information on the different completeness of the landslide maps.

4.3. Completeness of landslide inventories

Completeness is the degree to which an inventory is capable of recording all the landslides in an area, during a single event or in a period of time. Ideally, an inventory should record all landslides that have occurred in an area that left discernable features. However, features left by landslides may not be recognized in the field or through the interpretation of aerial photographs, as they are often obscured or cancelled by erosion, vegetation, urbanization, and human action, including ploughing. It is also possible that landslides occurred in remote areas

but were not reported because they did not cause damage. For these reasons, landslide inventories are generally incomplete.

Estimating the completeness of a landslide inventory is a difficult task, and considerations differ for archive, geomorphological, event and multi-temporal inventories. A formal definition of completeness requires that a landslide inventory includes all landslides associated with a landslide event (a single trigger) or multiple landslide events over time (geomorphological or multi-temporal). This definition assumes that all landslides are visible and recognizable, or that they were accurately reported, and that the entire study area affected, even marginally, by the trigger(s) is fully and thoroughly investigated. For practical reasons, these criteria are never met.

A functional definition of completeness requires that the landslide inventory includes a substantial fraction of all landslides at all scales. The tools and techniques available to compile the inventory must be able to meet this requirement within the study area. An important attribute of this definition is that a substantially complete inventory must include a substantial fraction of the smallest landslides. It is important to understand that the definition is applicable to landslide event inventories, but not to geomorphological inventories, because many smaller and intermediate-size landslides in geomorphological inventories have been erased by erosion and human action. Thus, a geomorphological inventory is always incomplete. This should be considered when determining landslide hazard and risk.

4.3.1. Completeness of archive inventories

Archive inventories are non-instrumental records of past events. Analysis of the information content of archive inventories of natural events is difficult and rarely pursued (Guzzetti *et al.*, 1994, 2005b,c; Ibsen and Brunsden, 1996; Glade, 1988; Guzzetti, 2000; Glade *et al.*, 2001; Guzzetti and Tonelli, 2004). An approach to evaluate the completeness of an archive inventory consists in the analysis of the cumulative number of historical landslide events. For a catalogue of historical events, the cumulative number of events is easily obtained by adding progressively the number of events recorded in each time interval (e.g., a day or a year).

Figure 4.9.A shows the temporal distribution of fatal landslide events in Italy, from 1500 to 2004. In this figure, the y-axis (logarithmic scale) shows the number of the consequences, i.e., fatalities (deaths and missing persons) and injured people. Also shown are events for which casualties occurred in unknown number. Inspection of the graph indicates that the distribution of the inventoried events varies substantially with time.

In an attempt to evaluate the completeness of this catalogue, in Figure 4.9.B I show the cumulative curves of fatal landslides events, in the period from 1410 to 2004. Inspection of Figure 4.9.B reveals that, as it might be expected, the cumulative number of landslide fatalities has increased largely since the beginning of the record, but also that the rates at which fatal events have occurred has increased. This may be a result of variations in the completeness of the historical catalogue. The more remote the period considered, the larger the number of events that probably remained unrecorded. This is especially evident for events that caused fewer than three fatalities. In the historical catalogue, such events rarely appear before 1800 (only 29 events). After 1800 they represent 30.5% of the total number of landslide events. The percentage increases to 73.4% after 1900. Even considering the increase in population that has occurred in Italy (Figure 1.2), there is no reason for the distribution of less catastrophic events to be so skewed, except for the incompleteness of the catalogue.

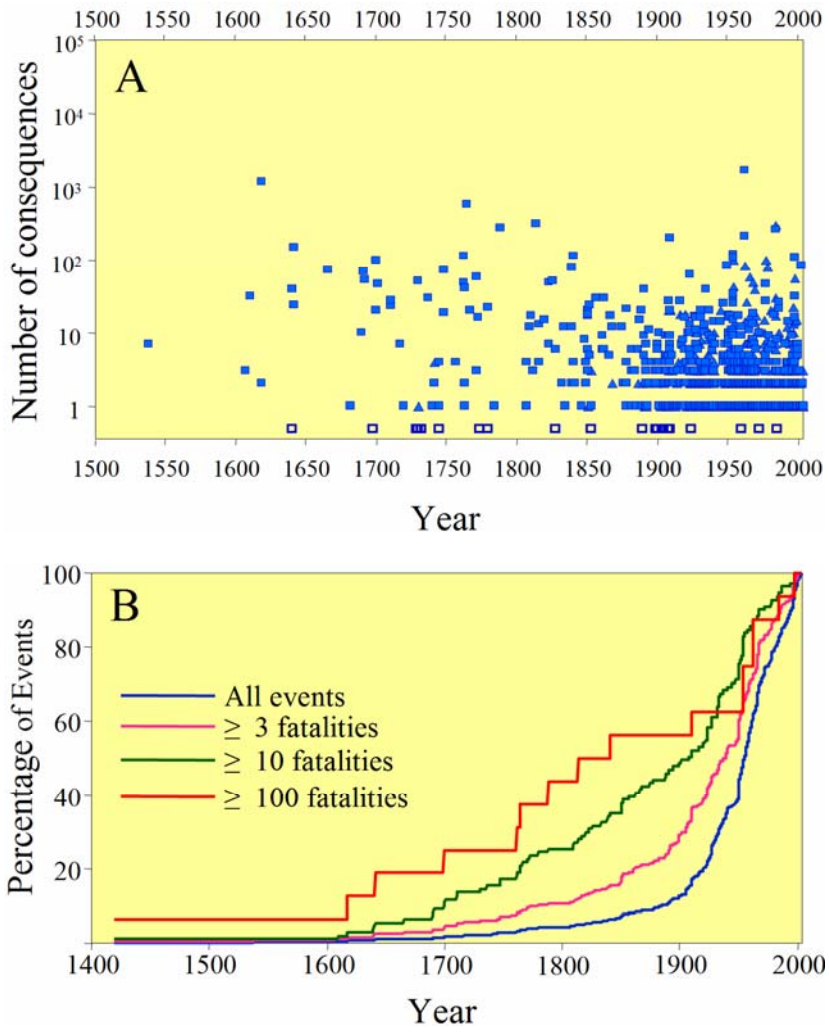

Figure 4.9 – Completeness of archive catalogue. (A) Historical distribution of damaging landslide events in Italy, form 1500 to 2004. Blue squares, fatalities; blue triangles, injured people; open squares, events for which casualties occurred in unknown number. (B) Cumulative distribution of landslide events that resulted in fatalities in Italy from 1410 to 2004. Blue line, all landslide events. Orange dashed line, low-intensity landslide events that resulted in three or more fatalities. Green line, medium-intensity landslide events that resulted in 10 or more fatalities. Red line, high-intensity landslide events with 100 or more fatalities.

In Figure 4.9.B, the blue line shows the yearly cumulative distribution of all events that resulted in at least one fatality. The slope of the curve increases sharply after ~ 1900. A second, less definite change in the slope of the curve occurs around 1690-1700. The other curves shown in Figure 4.9 represent yearly cumulative distributions of landslide events that resulted respectively in three or more (orange dashed line), ten or more (green line), and 100 or more (red line) landslide fatalities. The change in slope around 1900 is present in both the orange (≥ 3 fatalities) and green (≥ 10 fatalities) lines, but not in the red line (≥ 100 fatalities). However, it is less distinct in these curves than it is in the blue line. This indicates that the completeness of the historical catalogue varies with the intensity of the fatal events. For large-intensity events with at least 100 casualties the historical catalogue is probably complete for the period from 1600 to 2004. For medium-intensity (≥ 10 fatalities) and low-intensity (≥ 3) events the catalogue is reasonably complete only after ~ 1920. If all events are taken into

account, the catalogue can be considered almost complete for statistical purposes starting in 1920 and complete after 1950.

I now attempt to better quantify the described approach to evaluate the completeness of an historical catalogue. Assuming the cumulative number of historical events is a continuous and differentiable function (or it can be represented by a continuous and differentiable function), the slope of the cumulative curve is given by:

$$R_L = \frac{dN_L}{dt} \tag{4.4}$$

where N_L is the cumulative number of landslide events at time t, and dt is the time step used in the analysis (e.g., a year in Figure 4.9.B).

The slope of the cumulative curve is a measure of the rate of occurrence of the events. Assuming the rate of occurrence of the fatal events remains constant, i.e., $R_L = \lambda$, changes in the slope of the cumulative curve reflect – as a first approximation – differences in the completeness of the historical catalogue. Hence, if the slope of the cumulative curve remains constant for a given period, the catalogue is complete in that period. Conversely, if the degree of completeness varies, the slope of the cumulative curve changes accordingly.

The approach has undoubtedly limitations, as it makes the strong assumption that the processes that cause landslide fatalities remain constant for the considered period, i.e., that the rate and magnitude of the triggering events does not change in the period. Conditions leading to slope failures, such as climatic anomalies, rainfall events, land-use characteristics, and human actions, may change significantly over the time span of an historical catalogue, particularly if the latter extends for several decades or even centuries, invalidating the adopted assumption. Also, as shown in Figure 1.2, the population has increased substantially in the time span of the catalogue.

In a historical catalogue of landslide events the lack of occurrences in any given period may be due either to the catalogue's incompleteness or to variation in the conditions that led to slope failure. One has to assume that one (i.e., the rate of occurrence or the completeness) is known and remains constant, to estimate the other.

4.3.2. Completeness of geomorphological, event, and multi-temporal maps

The functional definition of completeness of a landslide inventory given before (§ 4.3) requires that the examined landslide map includes a substantial fraction of all landslides at all scales. This is very difficult to establish, and can only be inferred from external information.

In general, an event inventory map is more complete than a geomorphological inventory. Immediately following a landslide triggering event (i.e., a rainstorm, an earthquake or a snow melt event), individual landslides are usually clearly recognizable, in the field and on the aerial photographs, allowing for the production of complete (or nearly complete) event inventories. Landslide boundaries are usually distinct, making it relatively easy for the geomorphologist to identify and map the landslides. This is particularly true for shallow landslides, such as soil slides and debris flows. However, cases exist where some of the features typical of a landslide (e.g., the crown area, the lateral shear boundaries, or a bulging toe) may not be clearly identifiable for shallow landslides, particularly where the material did not mobilize after failure (Cardinali *et al*., 2000) (Figure 4.10). For large and complex slope movements, the boundary between the stable terrain and the failed mass is transitional and may change during

and immediately after an event. Establishing the exact location of the landslide boundary is difficult, often impossible based solely on surface morphological information (Figure 4.10). The problem may not be relevant when compiling small- to medium-scale event inventories, but becomes a problem in the preparation of large-scale event inventories. An error in mapping the boundary of a large landslide may affect significantly the measure of the size of the landslide, negatively affecting the frequency-area statistics that can be obtained from event inventory maps (§ 5).

Figure 4.10 – Deep-seated (left) and shallow (right) landslides in Umbria, showing difficulty in identifying and mapping the exact location of the boundary of a landslide, in the field or from aerial photographs.

Depending on the scale of the aerial photographs, small and very small landslides (with an area of a few tens of square meters) are more easily identified and mapped in the field, whereas medium, large and very large area landslides (e.g., extending for several hectares) are better identified and mapped from the aerial photographs. In a landslide mapping effort, field survey is often restricted to limited areas, along the roads, the divides or the rivers, depending on morphology. In these areas very small landslides can be mapped precisely, even if the area is wooded. In forested terrain precise location of the slope failures is a problem. Aerial photographs allow for a more complete coverage of the area affected by the triggering event, allowing for a more systematic (and complete) mapping, but may not be adequate for mapping accurately and methodically small landslides in forested terrain (Brardinoni *et al*., 2003).

Morphological features typical of landslides, including the boundaries, become increasingly indistinct with the age of the landslide (McCalpin, 1984). This is due to local adjustments of the landslides to reactivations and new slope failures, to surface erosion processes, and to human actions, including ploughing and land use changes. The rates at which landslide features disappear depend on many factors, such as the type, number and extent of the landslides, the number and magnitude of the triggering events, and the morphological and tectonic activity of the area. With time, the progressive disappearance of landslide features makes it much harder to identify them in the field and from aerial photographs. Disappearance of the landslide features is the primary reason for the incompleteness of geomorphological inventories. Even detailed geomorphological inventory maps may largely underestimate the actual number of landslides that have occurred in an area, which remains unknown. As I have discussed in § 3.3.4, multi-temporal inventory maps are prepared through the compilation of landslide information from different sources, and chiefly the interpretation of aerial photographs of different dates and periods. When multiple sets of aerial photographs are used,

the completeness of a multi-temporal inventory should be better than that of a corresponding geomorphological inventory map for the same area, but poorer than that of an event inventory. This hypothesis will be tested for the Collazzone area in § 5.3.1.

4.4. Landslide persistence

Landslide persistence is the degree to which new slope failures occur in the same place as existing landslides. Establishing landslide persistence has implications for landslide susceptibility and hazard assessment. The persistence of landslides can be established, and quantified, by comparing geomorphological, event, and multi-temporal inventory maps in a GIS.

For Umbria, information is available to attempt establishing quantitatively the persistence of landslides. Comparison in a GIS of the spatial distribution of landslides triggered by the 1937-1941 rainfall periods (§ 3.3.3.1) and by the January 1997 rapid snowmelt event (§ 3.3.3.2), with the geographical distribution of the pre-existing landslides shown in the detailed geomorphological inventory map (§ 3.3.2.2, Figure 3.10) allows for estimating the spatial persistence of landslides. Approximately 89% of all the rainfall induced landslides triggered in the period between 1937 and 1941 were located inside or within 150 metres from a pre-existing landslide (Figure 4.11.A). Similarly, about 75% of the snowmelt induced landslides in January 1997 fell inside pre-existing landslide deposits, i.e., they were reactivations, or they were located within 150 meters of an existing landslide (Figure 4.11.B). This is important information for the assessment of landslide susceptibility and hazards in Umbria, because it provides the rationale for attempting to evaluate where landslides may cause damage in the future based on where landslides have occurred in the past, using accurate landslide inventory maps.

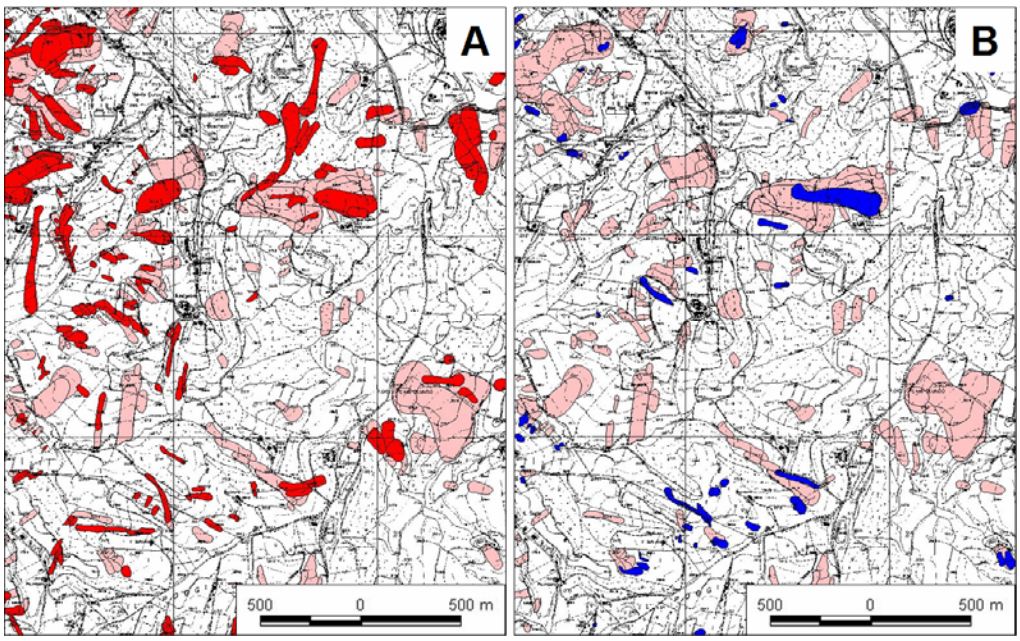

Figure 4.11 – Spatial persistence of event triggered landslides in Umbria. (A) Landslides triggered by intense and prolonged rainfall in the period between 1937 and 1941 (see § 3.3.3.1). (B) Landslides triggered by rapid snowmelt in January 1997 (see § 3.3.3.2). Legend: pink, pre-existing landslides (see § 3.3.2.1); red, 1937-41 landslides; blue, January 1997 landslides.

It should be noted that new landslides do not necessarily occur inside or in the vicinity of pre-existing landslide deposits. For the Staffora River basin, in the northern Apennines (§ 2.6), Guzzetti *et al*. (2005a) found low values of landslide persistence. By analysing a multi-temporal inventory map compiled through the systematic analysis of five sets of aerial photographs covering the period between 1955 and 1999, these authors found that in the Staffora basin 40% of all the landslides identified in the period from 1955 to 1999 occurred inside pre-existing landslides mapped on the 1955 aerial photographs. Considering only the landslides occurred in the 45-year period from 1955 to 1999, only 12% of the slope failures occurred in the same area of other landslides occurred in the same period. This is lower landslide persistence than the one observed in Umbria.

4.5. Temporal frequency of slope failures

The temporal frequency (or the recurrence) of landslide events can be established from archive inventories (Coe *et al.*, 2000; Guzzetti *et al.*, 2003a) and from multi-temporal landslide maps (Guzzetti *et al.*, 2005a). In § 7, I will show how to obtain information on the temporal probability of landslide events from a multi-temporal inventory map, and how to exploit this information to determine landslide hazard.

4.5.1. Exceedance probability of landslide occurrence

Before showing how to obtain the probability of landslide occurrence from archive inventories, it is convenient to establish an appropriate mathematical framework. As a first approximation, landslides can be considered as independent random point-events in time (Crovelli, 2000). In this framework, the exceedance probability of occurrence of landslide events during time t is:

$$P(N_L) = P\left[N_L(t) \geq 1\right] \tag{4.5}$$

where $N_L(t)$ is the number of landslides that occur during time t in the investigated area.

Two probability models are commonly used to investigate the occurrence of naturally occurring random point-events in time: (i) the Poisson model and (ii) the binomial model[1] (Crovelli, 2000; Önöz and Bayazit, 2001). The Poisson model is a continuous-time model consisting of random-point events that occur independently in ordinary time, which is considered naturally continuous. The Poisson model has been used to investigate the temporal occurrence of floods (Yevjevich, 1972; Önöz and Bayazit, 2001), volcanic eruptions (Klein, 1982; Connor and Hill, 1995; Nathenson, 2001) and landslides (Crovelli, 2000; Coe *et al.,* 2000; Roberds, 2005). Adopting a Poisson model for the temporal occurrence of landslides, the probability of experiencing n landslides during time t is given by

$$P[N_L(t) = n] = e^{(-\lambda t)} \frac{(\lambda t)^n}{n!} \quad n = 0, 1, 2, \ldots \tag{4.6}$$

[1] Other probability distributions used to model naturally occurring random point-events in time include the Weibull distribution (Bebbington and Lai, 1996) and the mixed exponential distribution (Cox and Lewis, 1966; Nathenson, 2001).

where λ is the estimated average rate of occurrence of landslides, which corresponds to 1/μ, with μ the estimated mean recurrence interval between successive failure events. The model parameters λ and μ can be obtained from a historical catalogue of landslide events or from a multi-temporal landslide inventory map.

From equation 4.6, the probability of experiencing one or more landslides during time *t* (i.e., the exceedance probability) is

$$P[N_L(t) \geq 1] = 1 - P[N_L(t) = 0] = 1 - e^{-\lambda t} = 1 - e^{-t/\mu} \tag{4.7}$$

Discussing equation 4.7, Crovelli (2000) noted that for a given period of time *t*, if $\mu \rightarrow \infty$, then $P[N_L(t) \geq 1] \rightarrow 0$, i.e., if the estimated mean recurrence interval between successive events is very large, chances are that no failures will be experienced in the considered period. Also, if the estimated mean recurrence μ is fixed, and the time interval is very long ($t \rightarrow \infty$), then $P[N_L(t) \geq 1] \rightarrow 1$ and one is certain to observe a landslide event.

The Poisson model allows for determining the probability of future landslides for different times *t* (i.e., for a different number of years) based on the statistics of past landslide events, under the following assumptions (Crovelli, 2000): (i) the number of landslide events which occur in disjoint time intervals are independent, (ii) the probability of an event occurring in a very short time is proportional to the length of the time interval, (iii) the probability of more than one event in a short time interval is negligible, (iv) the probability distribution of the number of events is the same for all time intervals of fixed length, and (v) the mean recurrence of events will remain the same in the future as it was observed in the past. These assumptions, which may not always hold for landslide events, should be considered when interpreting (and using) the results of the Poisson probability model.

As an alternative to the Poisson model, a binomial model can be adopted. The binomial probability model is a discrete-time model consisting of the occurrence or random-point events in time. In this model time is divided into discrete increments of equal length, and within each time increment a single point-event may or may not occur. The binomial model was adopted by Costa and Baker (1981) to investigate the occurrence of floods, and by Keaton *et al*. (1988), Lips and Wieczorek (1990), Coe *et al*. (2000), Raetso *et al*. (2002), and Vandine *et al*. (2004) to study the temporal occurrence of landslides and debris flows.

Following Crovelli (2000), and adopting the binomial probability model, the exceedance probability of experiencing one or more landslides during time *t* is

$$P[N_L(t) \geq 1] = 1 - P[N_L(t) = 0] = 1 - (1 - p)^t = 1 - (1 - 1/\mu)^t \tag{4.8}$$

where, *p* is the estimated probability of a landslide event in time *t*, and $\mu = 1/p$ is the estimated mean recurrence interval between successive slope failures. As for the Poisson model, μ can be obtained from a historical catalogue of landslide events or from a multi-temporal landslide inventory map. The binomial model holds under the same or similar assumptions listed for the Poisson model.

Crovelli (2000) compared the Poisson and the binomial probability models, and showed that the two models differ for short mean recurrence intervals (i.e., when μ is small) and for short periods of time (i.e., when *t* is small), with the binomial model over estimating the exceedance probability of future landslide events. For large periods of times and large mean recurrence intervals, the two models provide very similar or identical estimates of the probability of

future landslide occurrences. Indeed, it can be shown that when t and μ are large, the Poisson probability distribution approximates the binomial probability distribution.

4.5.1.1. Temporal probability of historical landslide events in Umbria

In this section, I exploit the information available on historical landslide events in Umbria to estimate the temporal probability of slope failures, for different periods. For the Umbria region, the AVI archive inventory of historical landslide events in Italy (§ 3.3.1.1, Figure 3.4) lists information on 1292 landslide sites, affected by a total of 1488 landslide events.

Considering the 85-year period from 1917 to 2001, most of the landslide sites (1158, i.e., 89.6%) were affected only once, 78 (7.6%) were affected two times, and 36 (2.8%) were affected three to six times. This information allows for computing the average recurrence of landslides in the 92 Municipalities in the Umbria region. Average recurrence can be computed by dividing the total number of landslide events in each Municipality by the time span of the catalogue (i.e., 85 years). Assuming that landslide recurrence will remain the same for the future (a "strong" geomorphological assumption that should always be tested, where possible) and adopting a Poisson probability model, the exceedance probability of having one or more damaging landslide event in each Municipality in Umbria can be determined for different time intervals. Results are shown in Figure 4.12 and summarised in Table 4.3.

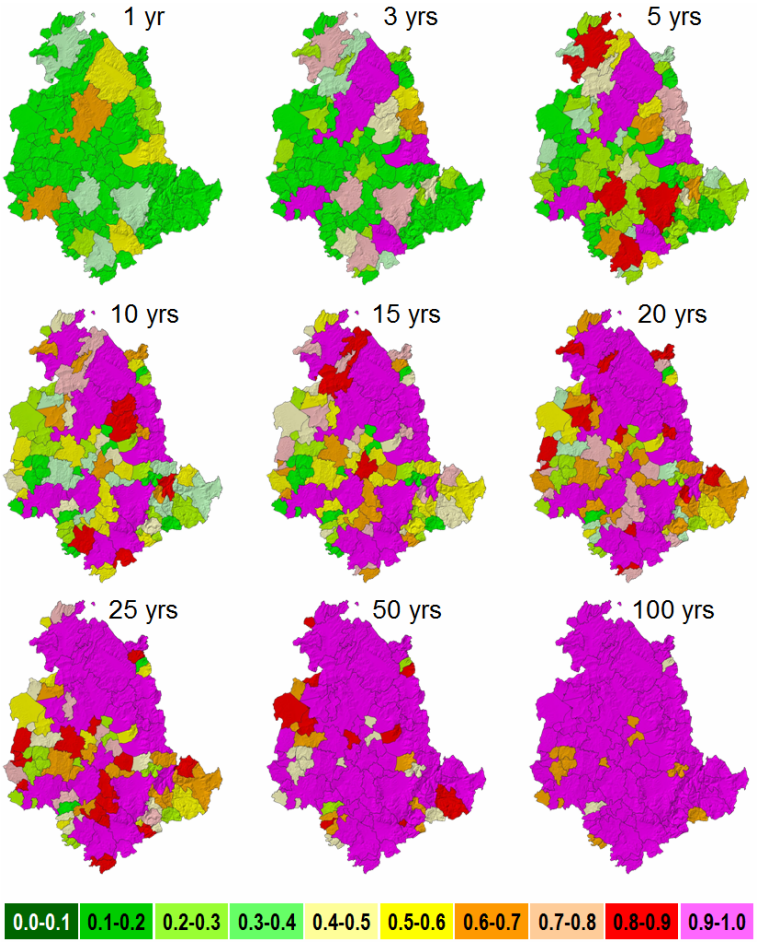

Figure 4.12 – Maps showing annual exceedance probability of damaging landslide events in the 92 Municipalities in the Umbria region. Exceedance probability computed based on historical information for the 85-year period between 1917 and 2001.

Inspection of Table 4.3 reveals that for a 5-year period only five Municipalities in Umbria (5.4%) have a 0.90 or larger probability of experiencing at least one damaging landslide, and 17 Municipalities (18.5%) have a 0.50 or larger probability of experiencing at least one damaging slope failure. These figures increase to 11 (12.0%) and 40 (43.5%) Municipalities for a 10-year period, and to 25 (27.2%) and 68 (73.9%) Municipalities for a 25-year period, respectively. After 100 years, all the Municipalities in Umbria have a 50% or larger probability of experiencing a landslide, and 76 Municipalities (82.6%) have a 90% or larger probability of having at least one slope failure (Figure 4.12).

Table 4.3 – Number and percentage (in parenthesis) of municipalities in Umbria that exceed the given probability of experiencing one or more damaging landslide. Values for different time intervals, from 5 to 50 years. Based on a historical record spanning the 85-year period between 1917 and 2001.

EXCEEDANCE PROBABILITY	*5 YRS*	*10 YRS*	*20 YRS*	*25 YRS*	*50 YRS*
> 0.99	2 (2.2%)	5 (5.4%)	11 (12.0%)	14 (15.2%)	25 (27.2%)
> 0.95	5 (5.4%)	10 (10.9%)	16 (17.4%)	18 (19.6%)	40 (43.5%)
> 0.90	5 (5.4%)	11 (12.0%)	19 (20.7%)	25 (27.2%)	58 (63.0%)
> 0.80	9 (9.8%)	16 (17.4%)	30 (32.6%)	40 (43.5%)	68 (73.9%)
> 0.50	17 (18.5)	40 (43.5%)	68 (73.9%)	68 (73.9%)	76 (82.6%)

4.6. Summary of achieved results

In this chapter, I have:

(a) Further demonstrated how to compare landslide maps, and to measure the quality and completeness of different landslide inventory maps.

(b) Proposed methods for the construction of landslide density maps, a weak proxy for susceptibility zonings where these are not available.

(c) Proposed methods for the analysis of the spatial persistence of slope failures, important information for landslide hazard and risk assessments.

(d) Shown how to obtain temporal information on landslides from archive inventories, including a measure of the completeness of the historical archives, essential information for probabilistic landslide hazard assessments.

This contributes to responds to Questions # 2 and # 3 posed in the Introduction (§ 1.2).